第一页为封面页

参赛队员姓名：吴松泽

中学：中国人民大学附属中学

省份：北京

国家/地区：中国

指导教师姓名：Miriam Rafailovich, Sunil K. Sharma

论文题目：Sustainable Nanocellulose Membranes for Proton Exchange Membrane Fuel Cells

第二页为创新性申明

本参赛团队声明所提交的论文是在指导老师指导下进行的研究工作和取得的研究成果。尽本团队所知，除了文中特别加以标注和致谢中所罗列的内容以外，论文中不包含其他人已经发表或撰写过的研究成果。若有不实之处，本人愿意承担一切相关责任。

参赛队员： 吴松泽

指导老师：Miriam Rafailovich, Sunil K. Sharma

2019 年 **9** 月 **13** 日

Sustainable Nanocellulose Membranes for Proton Exchange Membrane Fuel Cells

Songze Wu

High School Affiliated to Renmin University of China

ABSTRACT

Carboxycellulose nanofibers (CNFs) promise to be a sustainable and inexpensive alternative material for polymer electrolyte membranes (PEMs). However, its practical applications have been limited by its relatively low performance and reduced mechanical properties under typical operating conditions. In this study, citric acid cross-linked carboxycellulose nanofiber (CA/CNF) membranes were prepared by solvent casting method. Carboxycellulose nanofibers were derived from wood pulp by using chemical oxidation of hydroxyl group present on C6 position of the cellulose chain, and a chemical crosslink between the citric acid and CNF is revealed with Fourier Transform Infra-Red Spectrometry (FT-IR), Contact angle, and Thermogravimetric Analysis (TGA). The optimal fuel cell performance was obtained crosslinking 70 mL of 0.2 wt% CNF suspension with 0.3 mL of 1.0 M citric acid solution. The membrane electrode assemblies (MEAs), operated in oxygen atmosphere, exhibit maximum power density of 27.7 mW/cm^2 and maximum current density of 111.8 mA/cm^2 at 80 °C and 100% relative humidity for the CA/CNF membrane with 0.1 mg/cm^2 Pt loading on anode and cathode, which is approximately 30 times and 22 times better respectively than the uncrosslinked CNF film.

KEYWORDS

carboxycellulose, citric acid, PEMFCs, proton conductivity, nitro-oxidation, nanopapers

INTRODUCTION

With the mounting energy demands projected to increase by 50% or more by the next decade, we are consuming natural petroleum at a rate reported to be 105 times faster than nature can provide.[1,2] According to a 2009 prediction, current coal supplies can last for about 107 years, crude oil for about 35 years, and nature gas for about 37 years.[3] Such dependence on fossil fuels is not only unsustainable but also leads to climate change resulting from increasing greenhouse gas levels in the atmosphere.[4] Since it was proposed that global warming can be slowed and perhaps reversed only when society replaces fossil fuels with renewable, carbon-neutral alternatives, the search for ‘clean’ energy has become imperative.[5] Today, various renewable energy systems, such as direct solar,[6] photovoltaics,[7] wind,[8] geothermal,[9] and biomass,[10] have been intensively studied and extensively applied in real life. Among them, fuel cells, which convert chemical energy directly into electrical energy, are proposed as one of the promising alternative energy medium due to their high efficiency and low to zero emission.[11,12]

According to the electrolyte, the fuel cells are classified into seven categories: polymer electrolyte membrane fuel cell, including proton exchange membrane fuel cell (PEMFC), direct alcohol fuel cell (DAFC), anion exchange fuel cell (AEMFC); alkaline fuel cell (AFC); phosphoric acid fuel cell (PAFC); molten carbonate fuel cell (MCFC); and solid oxide fuel cell (SOFC).[11,13] Among various types of fuel cells, proton exchange membrane fuel cells (PEMFCs) are among the most promising energy conversion

devices because of their less extreme operating conditions, efficient power conversion, and utility in transportation.[14–16] Thus, PEMFCs have been developing most rapidly in the past decades.[17,18] Nafion, a perfluorinated sulfonic acid polymer produced by Du Pont, is a good proton conductor for hydrated membranes with long-term electrochemical stability and high mechanical strength.[15,19] However, Nafion membranes suffer from decreased conductivity and stability at high temperatures, excessive fuel crossover, and prohibitive high cost of US$ 800/m^2.[11,16,20–22] Therefore, several alternative materials with high performances and relatively lower cost have been developed as potential polymer electrolyte membranes (PEMs), including sulfonated poly(ether ether ketone),[16] polysulfone, [23] polybenzimidazole,[24] polyimide,[25] chitosan,[26] and alginate.[27]

Cellulose, the main component of cell walls of plants, algae, bacteria, and tunicates, is the most abundant biopolymer on our planet and has been used traditionally in many fields because it is renewabe, biocompatible, cheap, naturally biodegradable and chemically stable.[28,29] Recently, nanoscale cellulose materials have gained much interest thanks to their dimensional stability, low thermal expansion coefficient, outstanding reinforcing potential, and transparency as well as their nanoscale morphology, chemically tunable surface functionalities, ability to be obtained in various dimensions, and renewability.[30–32] According to the nomenclature proposed by the Technical Association of the Pulp and Paper Industry (TAPPI), nanocellulose can be classified into two main subcategories, cellulose nanocrystals (CNCs) and cellulose nanofibers (CNFs), based on size and aspect ratio.[33] In addition to its application in

fields such as nanofiltration,[34–36] solar cells,[37–39] and water purification,[40–42] nanocellulose have been widely applied in PEMs due to the low cost, excellent gas barrier properties, and acidic oxygen functional groups.[43] Previously, nanoellulose has been extensively used as a nanofiller to enhance the performance of Nafion and other conductive polymers.[16,44–47]

While the innate proton conductivity of nanocellulose is relatively low, various methods have been employed to enhance proton conductivity in nanocellulose-based materials. For example, Smolarkiewicz *et al.* prepared a nanocellulose film doped with imidazole as a “dry” electrolyte which exhibits nearly four orders of magnitude higher conductivity than a pure cellulose sample while maintaining thermal stability from 110 °C to 150 °C.[48] Bideau *et al.* synthesized a conductive nanocellulose-based film through grafting N-(3-aminopropyl)pyrrole onto oxidized CNF followed by oxidative polymerization of polypyrrole which improved the wettability, mechanical properties, thermal protection, and more importantly, the electrical conductivity by a factor of 105.[49] Jiang *et al.* prepared a PEM with improved power density from bacterial cellulose through incorporation of phosphoric acid (H_3PO_4/BC) and phytic acid (PA/BC) respectively, and found that acid-doping level of H_3PO_4/BC samples was higher than that of PA/BC membranes. However, the thermal stability, mechanical strength, and flexibility of PA/BC samples were better.[50] Bayer *et al.* reported nanocellulose membranes in which the proton conductivity increases up to 120 °C and with superior hydrogen barrier properties.[43] The maximum conductivity of CNF paper membranes was 0.05 mS cm^{-1} at 100 °C and that of CNC paper membranes was 4.6 mS cm^{-1} at

120 °C (both at 100% RH), and their power densities at 80 °C was 17 mW cm^{-2} and 0.8 mW cm^{-2} respectively.[43] Jankowska *et al.* found that all cellulose films showed similar thermal properties from room temperature to about 200 °C. However, the TEMPO-oxidized CNF film showed the highest proton conductivity of the samples studied, including non-oxidized CNF.[29] Recently, Guccini *et al.* evaluated the performance of thin carboxylated CNF-based membranes and obtained an optimized a proton conductivity exceeding 1 mS cm^{-1} at 30 °C between 65 and 95 % RH, only one order of magnitude lower than Nafion 212, while also exhibiting a lower hydrogen crossover than Nafion, despite being approximately 30 % thinner.[51]

While much progress has been made toward enhancing the proton conductivity of nanocellulose-based PEMs, other problems remain relatively unaddressed. As a hydrophilic film, one of nanocellulose's main limitations is its water sensitivity.[52] While the hydrophilic nature provides nanocellulose with excellent gas barrier properties, increasing ionic conductivity has been found to cause excessive water uptake, leading to a decrease of dimensional stability (i.e., high swelling).[53,54] While several methods of crosslinking to improve the mechanical properties have been developed, polycarboxylic acids, such as citric acid, have been identified as an effective strategy because of its environmental friendliness.[35,53,55,56] Previously, Dr. Sunil Sharma's group has developed a novel simple nitro-oxidation method to extract high aspect ratio carboxycellulose nanofibers, and the nanopaper prepared exhibited a tensile strength of 108 ± 2 MPa and a Young's modulus of 4.1 ± 0.2 GPa.[57,58] Thus, in this paper, we aim increase the

performance of CNF membrane fuel cells and improve the mechanical strength and stability of the membranes by citric acid crosslinking.

EXPERIMENTAL SECTION

Untreated wood pulp were provided by Stonybrook University. Analytical grade nitric acid (ACS reagent, 65%) and sodium nitrite (ACS reagent ≥ 97 %) were purchased from Sigma Aldrich; sodium bicarbonate was purchased from Fisher Scientific. Electrode of 0.1 mg/cm^2 Pt loading were purchased from FuelCellsEtc (College Station, Texas). H_2, N_2 and Air were purchased from Airgas (Radnor, PA). All chemicals were used without further purification.

Preparation of Carboxycellulose Nanofibers

Cellulose nanofibers were prepared from wood pulp via TEMPO oxidation process according to literature published earlier.[59,60] In this process, 10.0 g delignified wood pulp was well dispersed in about 500 mL of DI water. NaBr (1.0 g) and TEMPO reagent (0.20 g) were subsequently added into the dispersion stirrer for 15-20 min to make it homogeneous. The pH value of the reaction mixture was maintained 10.0 during the reaction process by slowely addition of 1 M NaOH solution. The oxidation process was initiated by adding 112.0 g NaOCl under continuous stirring for 20 h. There was frequent pH change was observed at the initial stages of the experiment, which is

due fast reaction, but it became less noticeable after a 3-4 hours. The reaction was quenched by adding 100 ml ethanol solution and stirring for 20 min vigorously. Cellulose fibers were separated by centrifugation at 7000 rpm along with washing 3 times with DI water. Finally, the product was placed in a dialysis bag until the conductivity of the medium was 5 μS. The concentration of the bulk cellulose nanofiber (CNF) suspension was measured to be 0.35 wt%.

Preparation of Citric Acid Crosslinked Carboxylcellulose Nanofibers

The citric acid crosslinked carboxylcellulose nanofibers (CA/CNF) were prepared by adding X mL of 1.0 M citric acid solution into 70.0 mL of as prepared CNF suspension diluted to 0.20 wt%(X = 0.050, 0.150, 0.300, 0.700, 1.400), and the resulting suspensions are denoted as CA/CNF-X respectively. CA/CNF membranes were prepared by the solvent evaporation method. In brief, a the CA/CNF suspensions was poured into a glass petri-dish and dried at 70 °C into a thin membrane. The membranes are then further dried under hot press at 110 °C (Approximately 230 °F) for 600 s. A membrane of CNF without citric acid is synthesized in a similar method without the addition of citric acid solution.

Fourier Transform Infra-Red Spectrometry (FTIR)

A Perkin Elmer Frontier FT-IR spectrometer with an Attenuated Total Reflectance accessory was used to record the FTIR curves in the transmission mode, between 700

and 4000 cm^{-1}. A total of 32 scans were taken per sample with a resolution of 4 cm^{-1}. The solid samples were recorded in the Attenuated Total Reflectance (ATR) mode.

Thermogravimetric Analysis (TGA)

The thermal stability of untreated raw wood, wood pulps and resulting carboxycellulose nanofibers membranes was studied by a Mettler Toledo TGA/SDTA851e instrument. Both TGA and differential thermogravimetry (DTG) curves were measured. The samples were run at a heating rate of 10 °C/min in the range of 35-800 °C under continuous nitrogen flow.

Contact Angle Measurement

Static water contact angles of CNF and CA/CNF films were measured using the KSV CAM 200 optical tensiometer. 5 μL of deionized water was then dropped onto the membrane using a micropipette. The contact angle of each membrane was measured 20 s after the drop deposition to ensure that the water droplet reached its equilibrium position. Each membrane was evaluated in triplicate to account for inhomogeneity.

Fuel Cell Testing

The single cell performance was evaluated on a fuel cell test station purchased from Fuel Cell Technologies, Inc. A commercial carbon cloth gas diffusion layer

electrode with a Pt loading of 0.1 mg/cm^2 was used at both the anode and cathode. The MEA was assembled by sandwiching the as prepared CNF and CA/CNF membranes between the electrodes and distributing the pressure uniformly across the MEA. The testing was performed using 99.99% pure H_2 with a flow rate of 50 sccm at the anode and 100 sccm of 99.99% pure O_2 at the cathode. The gases at both cathode and anode were heated to five degrees above operating temperature, to prevent condensation, and humidified to 100% relative humidity (RH). Testing was performed using an MEA assembly with an active area of 5 cm^2 at 80°C.

RESULTS AND DISCUSSION

Characterization of CA/CNF Membranes

The thermal degradation of the CNF and crosslinked CA/CNF membranes are characterized by TGA. As shown in Figure 1 (i), the residue weight of the uncrosslinked CNF, citric acid monohydrate, raw wood, and wood pulp are relatively insignificant compared to the approximately 20-30 % residue weight of CA/CNF membranes, which may be attributed to the fact that the addition of citric acid enhance the carbonization through increasing the carbon content of CA/CNF by ester bonding of citric acid molecules in the crosslink.[65] The DTG of the samples are as shown in Figure 1 (ii). For the raw wood and wood pulp samples, there were two major decomposition peaks at approximately 280 °C and 350 °C, which are in good agreement with agreement with previous literature and correspond to the degradation of hemicellulose and cellulose

respectively.[57,58,66] For the citric acid monohydrate, the degradation at around approximately 130 °C may be attributed to the loss of crystalline water while the second degradation at approximately 215 °C may be attributed to the thermal decomposition of citric acid. [67,68] While the initial degradation occurring around or below 100 °C may be attributed to the loss of physically adsorbed citric acid on the CNF and CA/CNF membranes, the peaks at approximately 250 °C and 300 °C may be attributed to the degradation of the anhydroglucoronic and anhydroglucose units in CNF respectively, and the lower degradation temperature compared to the raw wood and wood pulp reflects the nanoscale nature of CNF and CA/CNF.[58] In addition, for the CA/CNF-0.7 and CA/CNF-1.4, the degradation peak at approximately 190 °C can be observed but is absent in the CNF and CA/CNF samples with lower citric acid content. Upon further inspection, this degradation share a similar onset temperature of approximately 170 °C with the second degradation step of citric acid monohydrate. Thus, this degradation peak can be attributed to the degradation of the excess citric acid that is present in the CA/CNF samples with a higher CA/CNF content.[65,68] In other words, the citric acid crosslink has reached saturation in CA/CNF-0.7 and CA/CNF-1.4, and the excess citric acid exists as residuals in the solvent casted membrane.

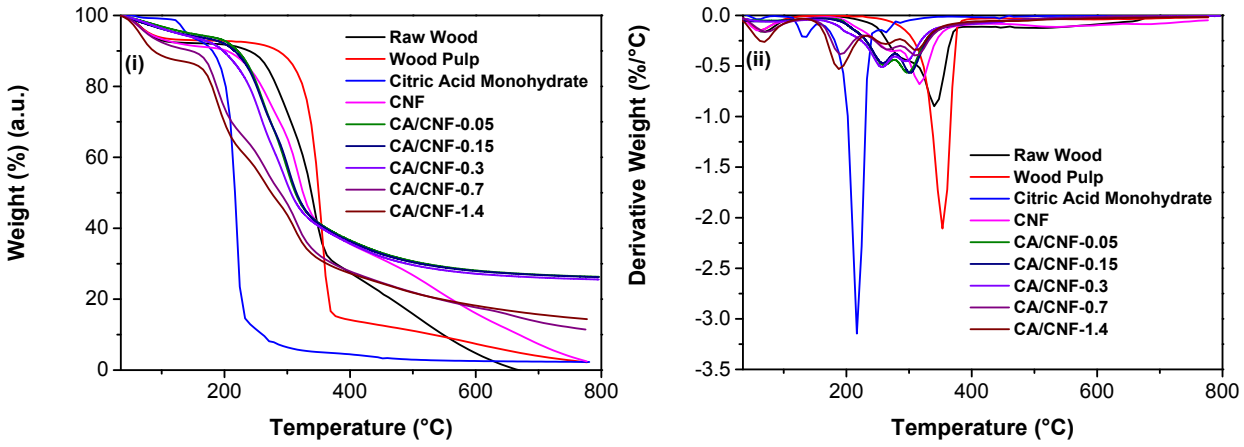

Figure 1. TGA and DTG graph of CA/CNF and original material

Figure 2 shows the FT-IR spectra of CNF and CA/CNF membranes as well as other references samples. For raw wood and wood pulp, the peak at approximately 1058 cm^{-1} may be attributed to the C-O stretching vibration mainly from the cellulose C-O bonds, and this peak is also similarly present in the CNF and CA/CNF samples.[57,58] For the uncrosslinked CNF and the crosslinked CA/CNF membranes, the peaks at approximately 3342 cm^{-1}, 2902 cm^{-1}, and 1317 cm^{-1} may be attributed to the O-H stretching, C-H stretching, and C-H bending respectively.[28,35,58,65,67,69] Moreover, the intensity of the C=O stretching peak at approximately 1716 cm^{-1} is found to increase from the uncrosslinked CNF membranes to the crosslinked CA/CNF membranes with the increase of amount of citric acid used in the solvent casting process. While the presence of the carboxyl in the uncrosslinked CNF membrane may be attributed to the carboxylic acid (-COOH) groups from the chemical oxidation of hydroxyl on C6 position, the increase in intensity may be attributed to the increasing content of O=H vibration in carboxylic acid and the ester formed in crosslinks in the CA/CNF membranes as the citric acid monohydrate also demonstrates a strong peak of C=O stretching in -COOH groups at approximately 1724 cm^{-1}.[35,65,67,70]

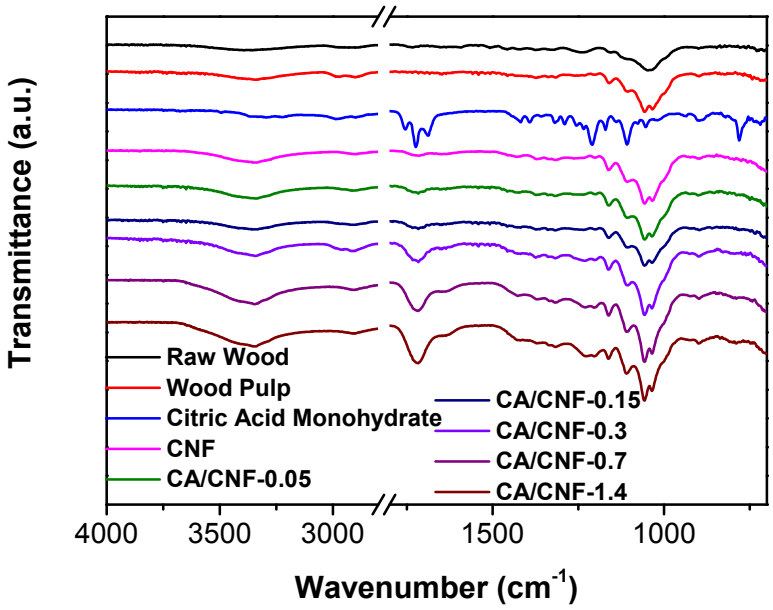

Figure 2. FTIR data for all samples of CA/CNF and raw material

Figure 3 shows contact angle measurements. The hydrophobicity of a membrane can be determined through the contact angle test: the larger the angle, the more hydrophobic the membrane is, and vice versa. Contact angle was measured and obtained for uncrosslinked CNF, CA/CNF-0.050, CA/CNF-0.150, CA/CNF-0.300, CA/CNF-0.700, and CA/CNF-1.400. It can be seen from the trend that hydrophobicity of CA/CNF decreases as citric acid concentration increases. In particular, the addition of 0.050 ml of 1M citric acid (as mentioned in the experiment section) resulted in a 9.8% decrease from 46.61° to 42.99°. This decrease in hydrophobicity represents an increase in the polarity of CA/CNF, which evidences the crosslinking of citric acid resulted in an increase of carboxyl and ester groups. An increase in carboxyl groups would result in an increase in fuel cell performance, as negatively charged tunnels are the primary way protons permeate the membrane.[35,43]

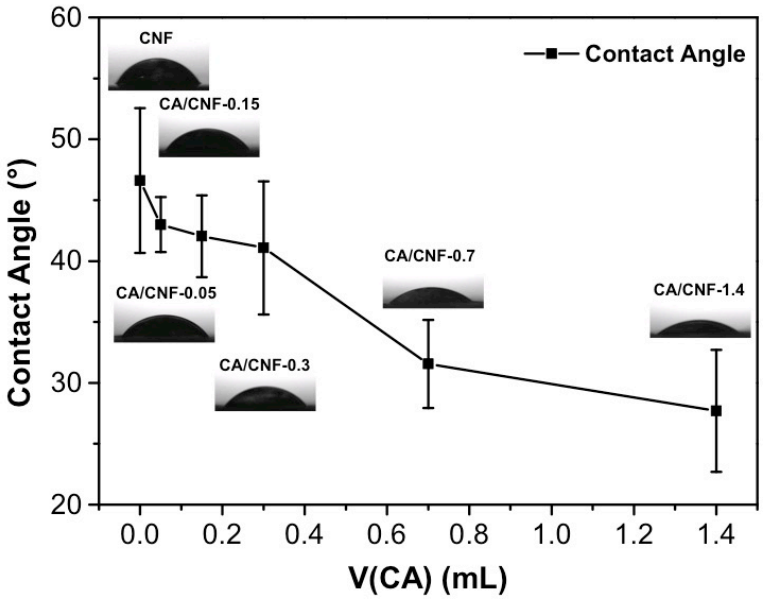

Figure 3. Contact angle data for all samples of CA/CNF**.**

Fuel Cell Performance

The CACNF and CNF membrane MEAs were evaluated on the fuel cell test station and the resulting polarization curves are shown in Figure 4. The control CNF membrane had an open circuit voltage (OCV) of 0.58 V. While this value lower than previously reported (32 μm thickness, 0.97 V), the CNF membrane as prepared here is significantly thicker (~75 μm thickness), thus increasing resistance and decreasing the OCV.[43,51] On the other hand, the CA/CNF membranes demonstrate a significantly enhanced OCV of approximately 0.75 V compared to the uncrosslinked CNF, which may be attributed to the fact that the CA crosslinking creates a more uniformly dense, less porous membrane that reduces hydrogen crossover, increasing the OCV. At 80 °C and 100% RH, the maximum current densities obtained for each membrane are shown in Figure 5 (i), with the highest maximum current density of 111.8 mA/cm^2 obtained with

the CA/CNF-0.3. Likewise, the maximum power densities obtained for each membrane are shown in Figure 5 (ii), with the highest maximum power density of 27.7 mW/cm^2 also obtained with the CA/CNF-0.3. Compared to the uncrosslinked CNF, which had a maximum current density of 5.0 mA/cm^2 and a maximum power density of 0.91 mW/cm^2, CA/CNF-0.3 achieved a 22 times increase in current density and 30 times increase in maximum power density. With the varying quantities of CA added, there was an initial improvement in performance parameters up until 0.3 mL 1.0 M CA, after which the performance declined with further increase of CA addition. The literature has previously demonstrated that a similar effect occurs when increasing the amount of phosphoric acid and phytic acid dopant in bacterial cellulose membranes, as the excess dopant, or crosslinkage in the case of CA, reduces the degree of freedom of ion transport and proton mobility.[50,71] Higher performances might be achieved with further tuning of the quantity of CA added and creating thinner membranes to lower resistance. Other crosslinking chemicals may be explored, possibly with more and stronger acidic groups.

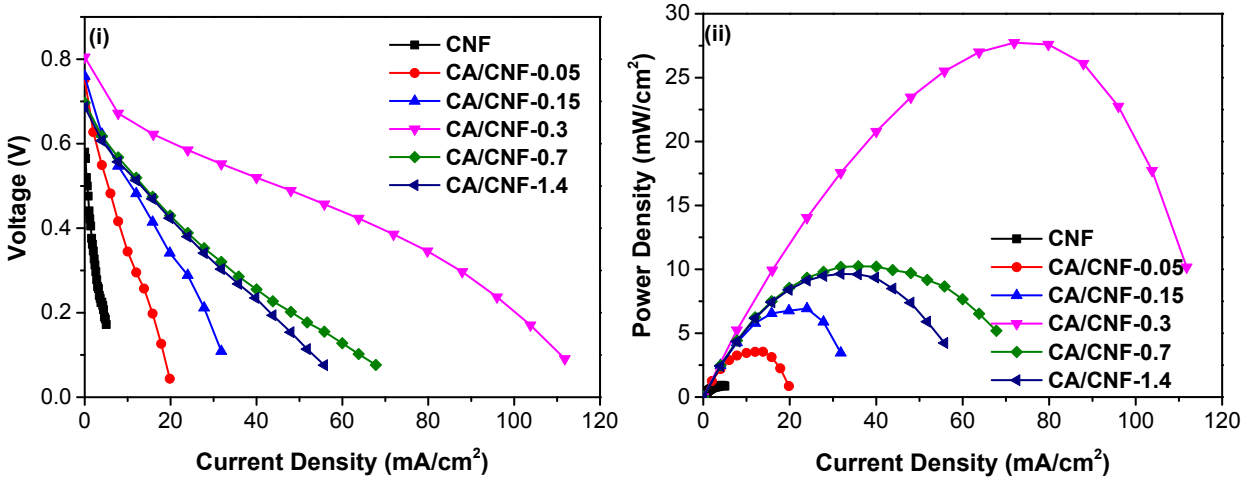

Figure 4. Polarization curves of all samples

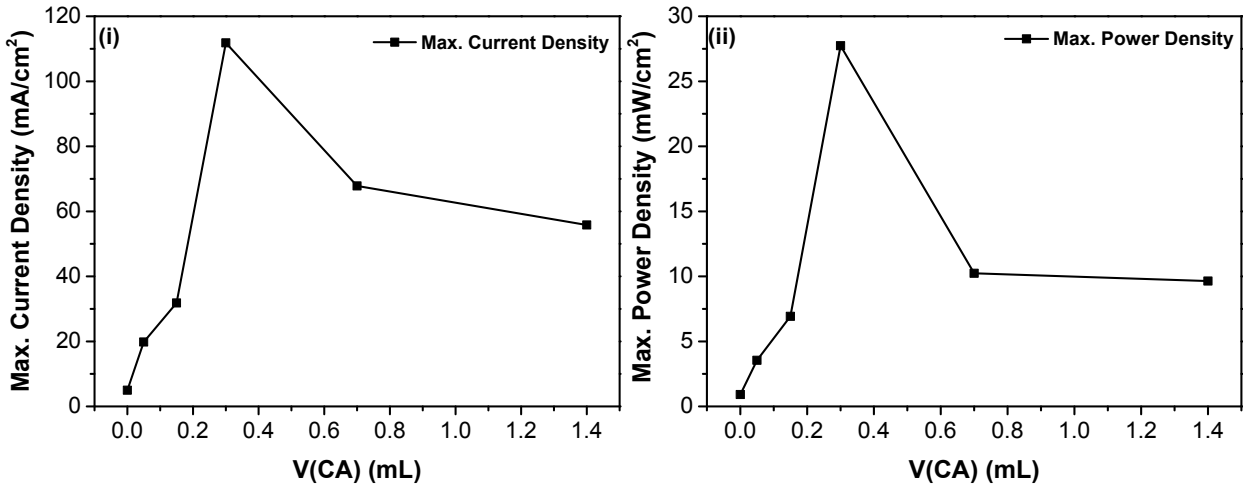

Figure 5. Trend of maximum power density and maximum current density.

CONCLUSION

The use of citric acid to crosslink CNF membranes is successful in enhancing the membrane's performance in PEM fuel cells. In this study, caboxycellulose nanofibers (CNF) was prepared from cellulose extracted from raw wood, and membranes were prepared using the solvent casting method. The citric acid crosslinked CNF membrane (CA/CNF) exhibited maximum power density of 27.7 mW/cm^2 and maximum current density of 111.8 mA/cm^2 at 80 °C and 100% relative humidity with 0.1 mg/cm^2 Pt loading on anode and cathode. The power density and current density results are approximately 30 times and 22 times better respectively than the uncrosslinked CNF film. Contact angle, TGA, and FTIR characterizations all demonstrate that CA/CNF has more carboxylic acid groups than uncrosslinked CNF, which, according to previous research, may be the reason for this increase in fuel cell performance. This work shows that CNF, when crosslinked with citric acid, has the potential of becoming a green and

environmentally friendly material that can be used as membranes in PEM fuel cells. Future research is needed to test the practical applications of CA/CNF, and also to evaluate the effects of other chemicals that could be used to crosslink CNF.

ACKNOWLEDGMENTS

This research project was conducted during the Garcia Summer Research Program 2019, a summer research program in Stonybrook University, New York, for talented high school students interested in research. The research would have been impossible without the help of my mentors at Garcia, Professor Miriam Rafailovich and Dr. Sunil K. Sharma. The background of this research was based on the previous research of Dr. Sunil K. Sharma, who developed a new method of preparing CNF and investigated in its properties.

REFERENCES

(1) Maness P, Y. J. E. C. G. M. Photobiological Hydrogen Production – Prospects and Challenges. *Microbe Mag.* **2009**, *4* (6), 275–280. https://doi.org/10.1128/microbe.4.275.1.

(2) Netravali, A. N.; Chabba, S. Composites Get Greener. *Mater. Today* **2003**, *6* (4), 22–29. https://doi.org/10.1016/S1369-7021(03)00427-9.

(3) Shafiee, S.; Topal, E. When Will Fossil Fuel Reserves Be Diminished? *Energy Policy* **2009**, *37* (1), 181–189. https://doi.org/10.1016/j.enpol.2008.08.016.

(4) Rittmann, B. E. Opportunities for Renewable Bioenergy Using Microorganisms. *Biotechnol. Bioeng.* **2008**, *100* (2), 203–212. https://doi.org/10.1002/bit.21875.

(5) Chisti, Y. Biodiesel from Microalgae. *Biotechnol. Adv.* **2007**, *25* (3), 294–306. https://doi.org/10.1016/j.biotechadv.2007.02.001.

(6) Vignarooban, K.; Xu, X.; Arvay, A.; Hsu, K.; Kannan, A. M. Heat Transfer Fluids for Concentrating Solar Power Systems – A Review. *Appl. Energy* **2015**, *146*, 383–396. https://doi.org/10.1016/j.apenergy.2015.01.125.

(7) Breyer, C.; Bogdanov, D.; Gulagi, A.; Aghahosseini, A.; Barbosa, L. S. N. S.; Koskinen, O.; Barasa, M.; Caldera, U.; Afanasyeva, S.; Child, M.; et al. On the Role of Solar Photovoltaics in Global Energy Transition Scenarios. *Prog. Photovoltaics Res. Appl.* **2017**, *25* (8), 727–745. https://doi.org/10.1002/pip.2885.

(8) Colmenar-Santos, A.; Perera-Perez, J.; Borge-Diez, D.; DePalacio-Rodríguez, C. Offshore Wind Energy: A Review of the Current Status, Challenges and Future Development in Spain. *Renew. Sustain. Energy Rev.* **2016**, *64*, 1–18. https://doi.org/10.1016/j.rser.2016.05.087.

(9) Shortall, R.; Davidsdottir, B.; Axelsson, G. Geothermal Energy for Sustainable Development: A Review of Sustainability Impacts and Assessment Frameworks. *Renew. Sustain. Energy Rev.* **2015**, *44*, 391–406. https://doi.org/10.1016/j.rser.2014.12.020.

(10) Nunes, L. J. R.; Matias, J. C. O.; Catalão, J. P. S. Biomass Combustion Systems: A Review on the Physical and Chemical Properties of the Ashes. *Renew. Sustain. Energy Rev.* **2016**, *53*, 235–242. https://doi.org/10.1016/j.rser.2015.08.053.

(11) Zhang, H.; Shen, P. K. Advances in the High Performance Polymer Electrolyte Membranes for Fuel Cells. *Chem. Soc. Rev.* **2012**, *41* (6), 2382–2394. https://doi.org/10.1039/C2CS15269J.

(12) Cheng, J.; He, G.; Zhang, F. A Mini-Review on Anion Exchange Membranes for Fuel Cell Applications: Stability Issue and Addressing Strategies. *Int. J. Hydrogen Energy* **2015**, *40* (23), 7348–7360. https://doi.org/10.1016/j.ijhydene.2015.04.040.

(13) Kim, D. J.; Jo, M. J.; Nam, S. Y. A Review of Polymer–Nanocomposite Electrolyte Membranes for Fuel Cell Application. *J. Ind. Eng. Chem.* **2015**, *21*, 36–52. https://doi.org/10.1016/j.jiec.2014.04.030.

(14) Merle, G.; Wessling, M.; Nijmeijer, K. Anion Exchange Membranes for Alkaline Fuel Cells: A Review. *J. Memb. Sci.* **2011**, *377* (1), 1–35. https://doi.org/10.1016/j.memsci.2011.04.043.

(15) Tsai, J.-C.; Cheng, H.-P.; Kuo, J.-F.; Huang, Y.-H.; Chen, C.-Y. Blended Nafion®/SPEEK Direct Methanol Fuel Cell Membranes for Reduced Methanol Permeability. *J. Power Sources* **2009**, *189* (2), 958–965. https://doi.org/10.1016/j.jpowsour.2008.12.071.

(16) Zhao, Q.; Wei, Y.; Ni, C.; Wang, L.; Liu, B.; Liu, J.; Zhang, M.; Men, Y.; Sun, Z.; Xie, H.; et al. Effect of Aminated Nanocrystal Cellulose on Proton Conductivity and Dimensional Stability of Proton Exchange Membranes. *Appl. Surf. Sci.* **2019**, *466* (October 2018), 691–702. https://doi.org/10.1016/j.apsusc.2018.10.063.

(17) Yan, Q.; Toghiani, H.; Causey, H. Steady State and Dynamic Performance of Proton Exchange Membrane Fuel Cells (PEMFCs) under Various Operating Conditions and Load Changes. *J. Power Sources* **2006**, *161* (1), 492–502. https://doi.org/10.1016/j.jpowsour.2006.03.077.

(18) Barbir, F.; Gómez, T. Efficiency and Economics of Proton Exchange Membrane (PEM) Fuel Cells. *Int. J. Hydrogen Energy* **1997**, *22* (10), 1027–1037. https://doi.org/10.1016/S0360-3199(96)00175-9.

(19) Wong, C. Y.; Wong, W. Y.; Ramya, K.; Khalid, M.; Loh, K. S.; Daud, W. R. W.; Lim, K. L.; Walvekar, R.; Kadhum, A. A. H. Additives in Proton Exchange Membranes for Low- and High-Temperature Fuel Cell Applications: A Review. *Int. J. Hydrogen Energy* **2019**, *44* (12), 6116–6135. https://doi.org/10.1016/j.ijhydene.2019.01.084.

(20) Alberti, G.; Casciola, M.; Massinelli, L.; Bauer, B. Polymeric Proton Conducting Membranes for Medium Temperature Fuel Cells (110–160°C). *J. Memb. Sci.* **2001**, *185* (1), 73–81. https://doi.org/10.1016/S0376-7388(00)00635-9.

(21) Yee, R. S. L.; Rozendal, R. A.; Zhang, K.; Ladewig, B. P. Cost Effective Cation Exchange Membranes: A Review. *Chem. Eng. Res. Des.* **2012**, *90* (7), 950–959. https://doi.org/10.1016/j.cherd.2011.10.015.

(22) Wilberforce, T.; Alaswad, A.; Palumbo, A.; Dassisti, M.; Olabi, A. G. Advances in Stationary and Portable Fuel Cell Applications. *Int. J. Hydrogen Energy* **2016**, *41* (37), 16509–16522. https://doi.org/10.1016/j.ijhydene.2016.02.057.

(23) Zhang, L.; Chen, G.; Tang, H.; Cheng, Q.; Wang, S. Preparation and Characterization of Composite Membranes of Polysulfone and Microcrystalline Cellulose. *J. Appl. Polym. Sci.* **2009**, *112* (1), 550–556. https://doi.org/10.1002/app.29434.

(24) Chuang, S.-W.; Hsu, S. L.-C. Synthesis and Properties of a New Fluorine-Containing Polybenzimidazole for High-Temperature Fuel-Cell Applications. *J. Polym. Sci. Part A Polym. Chem.* **2006**, *44* (15), 4508–4513. https://doi.org/10.1002/pola.21555.

(25) Asano, N.; Aoki, M.; Suzuki, S.; Miyatake, K.; Uchida, H.; Watanabe, M. Aliphatic/Aromatic Polyimide Ionomers as a Proton Conductive Membrane for Fuel Cell Applications. *J. Am. Chem. Soc.* **2006**, *128* (5), 1762–1769. https://doi.org/10.1021/ja0571491.

(26) Mukoma, P.; Jooste, B. R.; Vosloo, H. C. M. Synthesis and Characterization of Cross-Linked Chitosan Membranes for Application as Alternative Proton Exchange Membrane Materials in Fuel Cells. *J. Power Sources* **2004**, *136* (1), 16–23. https://doi.org/10.1016/j.jpowsour.2004.05.027.

(27) Smitha, B.; Sridhar, S.; Khan, A. A. Chitosan–Sodium Alginate Polyion Complexes as Fuel Cell Membranes. *Eur. Polym. J.* **2005**, *41* (8), 1859–1866. https://doi.org/10.1016/j.eurpolymj.2005.02.018.

(28) Sun, X.; Wu, Q.; Ren, S.; Lei, T. Comparison of Highly Transparent All-Cellulose Nanopaper Prepared Using Sulfuric Acid and TEMPO-Mediated Oxidation Methods. *Cellulose* **2015**, *22* (2), 1123–1133. https://doi.org/10.1007/s10570-015-0574-6.

(29) Jankowska, I.; Pankiewicz, R.; Pogorzelec-Glaser, K.; Ławniczak, P.; Łapiński, A.; Tritt-Goc, J. Comparison of Structural, Thermal and Proton Conductivity Properties of Micro- and Nanocelluloses. *Carbohydr. Polym.* **2018**, *200*, 536–542. https://doi.org/10.1016/j.carbpol.2018.08.033.

(30) Mohd Amin, K. N.; Annamalai, P. K.; Morrow, I. C.; Martin, D. Production of Cellulose Nanocrystals via a Scalable Mechanical Method. *RSC Adv.* **2015**, *5* (70), 57133–57140. https://doi.org/10.1039/c5ra06862b.

(31) Kim, J.-H.; Shim, B. S.; Kim, H. S.; Lee, Y.-J.; Min, S.-K.; Jang, D.; Abas, Z.; Kim, J. Review of Nanocellulose for Sustainable Future Materials. *Int. J. Precis. Eng. Manuf. Technol.* **2015**, *2* (2), 197–213. https://doi.org/10.1007/s40684-015-0024-9.

(32) Moon, R. J.; Martini, A.; Nairn, J.; Simonsen, J.; Youngblood, J. Cellulose Nanomaterials Review: Structure, Properties and Nanocomposites. *Chem. Soc. Rev.* **2011**, *40* (7), 3941–3994. https://doi.org/10.1039/C0CS00108B.

(33) Kargarzadeh, H.; Mariano, M.; Gopakumar, D.; Ahmad, I.; Thomas, S.; Dufresne, A.; Huang, J.; Lin, N. Advances in Cellulose Nanomaterials. *Cellulose* **2018**, *25* (4), 2151–2189. https://doi.org/10.1007/s10570-018-1723-5.

(34) Mautner, A.; Lee, K.-Y.; Lahtinen, P.; Hakalahti, M.; Tammelin, T.; Li, K.; Bismarck, A. Nanopapers for Organic Solvent Nanofiltration. *Chem. Commun.* **2014**, *50* (43), 5778–5781. https://doi.org/10.1039/C4CC00467A.

(35) Quellmalz, A.; Mihranyan, A. Citric Acid Cross-Linked Nanocellulose-Based Paper for Size-Exclusion Nanofiltration. *ACS Biomater. Sci. Eng.* **2015**, *1* (4), 271–276. https://doi.org/10.1021/ab500161x.

(36) Metreveli, G.; Wågberg, L.; Emmoth, E.; Belák, S.; Strømme, M.; Mihranyan, A. A Size-Exclusion Nanocellulose Filter Paper for Virus Removal. *Adv. Healthc. Mater.* **2014**, *3* (10), 1546–1550. https://doi.org/10.1002/adhm.201300641.

(37) Fang, Z.; Zhu, H.; Yuan, Y.; Ha, D.; Zhu, S.; Preston, C.; Chen, Q.; Li, Y.; Han, X.; Lee, S.; et al. Novel Nanostructured Paper with Ultrahigh Transparency and Ultrahigh Haze for Solar Cells. *Nano Lett.* **2014**, *14* (2), 765–773. https://doi.org/10.1021/nl404101p.

(38) Gao, L.; Chao, L.; Hou, M.; Liang, J.; Chen, Y.; Yu, H.-D.; Huang, W. Flexible, Transparent Nanocellulose Paper-Based Perovskite Solar Cells. *npj Flex. Electron.* **2019**, *3* (1), 4. https://doi.org/10.1038/s41528-019-0048-2.

(39) Costa, S. V.; Pingel, P.; Janietz, S.; Nogueira, A. F. Inverted Organic Solar Cells Using Nanocellulose as Substrate. *J. Appl. Polym. Sci.* **2016**, *133* (28). https://doi.org/10.1002/app.43679.

(40) Sharma, P. R.; Chattopadhyay, A.; Sharma, S. K.; Hsiao, B. S. Efficient Removal of UO22+ from Water Using Carboxycellulose Nanofibers Prepared by the Nitro-Oxidation Method. *Ind. Eng. Chem. Res.* **2017**, *56* (46), 13885–13893. https://doi.org/10.1021/acs.iecr.7b03659.

(41) Sharma, P. R.; Chattopadhyay, A.; Sharma, S. K.; Geng, L.; Amiralian, N.; Martin, D.; Hsiao, B. S. Nanocellulose from Spinifex as an Effective Adsorbent to Remove Cadmium(II) from Water. *ACS Sustain. Chem. Eng.* **2018**, *6* (3), 3279–3290. https://doi.org/10.1021/acssuschemeng.7b03473.

(42) Sharma, P. R.; Chattopadhyay, A.; Zhan, C.; Sharma, S. K.; Geng, L.; Hsiao, B. S. Lead Removal from Water Using Carboxycellulose Nanofibers Prepared by Nitro-Oxidation Method. *Cellulose* **2018**, *25* (3), 1961–1973. https://doi.org/10.1007/s10570-018-1659-9.

(43) Bayer, T.; Cunning, B. V.; Selyanchyn, R.; Nishihara, M.; Fujikawa, S.; Sasaki, K.; Lyth, S. M. High Temperature Proton Conduction in Nanocellulose Membranes: Paper Fuel Cells. *Chem. Mater.* **2016**, *28* (13), 4805–4814. https://doi.org/10.1021/acs.chemmater.6b01990.

(44) Jiang, G.; Zhang, J.; Qiao, J.; Jiang, Y.; Zarrin, H.; Chen, Z.; Hong, F. Bacterial Nanocellulose/Nafion Composite Membranes for Low Temperature Polymer Electrolyte Fuel Cells. *J. Power Sources* **2015**, *273*, 697–706. https://doi.org/10.1016/j.jpowsour.2014.09.145.

(45) Gadim, T. D. O.; Vilela, C.; Loureiro, F. J. A.; Silvestre, A. J. D.; Freire, C. S. R.; Figueiredo, F. M. L. Nafion® and Nanocellulose: A Partnership for Greener Polymer Electrolyte Membranes. *Ind. Crops Prod.* **2016**, *93*, 212–218. https://doi.org/10.1016/j.indcrop.2016.01.028.

(46) Hasani-Sadrabadi, M. M.; Dashtimoghadam, E.; Nasseri, R.; Karkhaneh, A.; Majedi, F. S.; Mokarram, N.; Renaud, P.; Jacob, K. I. Cellulose Nanowhiskers to Regulate the Microstructure of Perfluorosulfonate Ionomers for High-Performance Fuel Cells. *J. Mater. Chem. A* **2014**, *2* (29), 11334–11340. https://doi.org/10.1039/C4TA00635F.

(47) Ni, C.; Wei, Y.; Zhao, Q.; Liu, B.; Sun, Z.; Gu, Y.; Zhang, M.; Hu, W. Novel Proton Exchange Membranes Based on Structure-Optimized Poly(Ether Ether Ketone Ketone)s and Nanocrystalline Cellulose. *Appl. Surf. Sci.* **2018**, *434*, 163–175. https://doi.org/10.1016/j.apsusc.2017.09.094.

(48) Smolarkiewicz, I.; Rachocki, A.; Pogorzelec-Glasser, K.; Pankiewicz, R.; Ławniczak, P.; Łapiński, A.; Jarek, M.; Tritt-Goc, J.; Pogorzelec-Glaser, K.; Pankiewicz, R.; et al. Proton-Conducting Microcrystalline Cellulose Doped with Imidazole. Thermal and Electrical

Properties. *Electrochim. Acta* **2015**, *155*, 38–44. https://doi.org/110.1016/j.electacta.2014.11.205.

(49) Bideau, B.; Cherpozat, L.; Loranger, E.; Daneault, C. Conductive Nanocomposites Based on TEMPO-Oxidized Cellulose and Poly(N-3-Aminopropylpyrrole-Co-Pyrrole). *Ind. Crops Prod.* **2016**, *93*, 136–141. https://doi.org/10.1016/j.indcrop.2016.06.003.

(50) Jiang, G.; Qiao, J.; Hong, F. Application of Phosphoric Acid and Phytic Acid-Doped Bacterial Cellulose as Novel Proton-Conducting Membranes to PEMFC. *Int. J. Hydrogen Energy* **2012**, *37* (11), 9182–9192. https://doi.org/10.1016/j.ijhydene.2012.02.195.

(51) Guccini, V.; Carlson, A.; Yu, S.; Lindbergh, G.; Lindström, R. W.; Salazar-Alvarez, G. Highly Proton Conductive Membranes Based on Carboxylated Cellulose Nanofibres and Their Performance in Proton Exchange Membrane Fuel Cells. **2019**. https://doi.org/10.26434/chemrxiv.7851461.v3.

(52) Coma, V.; Sebti, I.; Pardon, P.; Pichavant, F. H.; Deschamps, A. Film Properties from Crosslinking of Cellulosic Derivatives with a Polyfunctional Carboxylic Acid. *Carbohydr. Polym.* **2003**, *51* (3), 265–271. https://doi.org/10.1016/S0144-8617(02)00191-1.

(53) Azeredo, H. M. C.; Kontou-Vrettou, C.; Moates, G. K.; Wellner, N.; Cross, K.; Pereira, P. H. F.; Waldron, K. W. Wheat Straw Hemicellulose Films as Affected by Citric Acid. *Food Hydrocoll.* **2015**, *50*, 1–6. https://doi.org/10.1016/j.foodhyd.2015.04.005.

(54) Lu, Y.; Armentrout, A. A.; Li, J.; Tekinalp, H. L.; Nanda, J.; Ozcan, S. A Cellulose Nanocrystal-Based Composite Electrolyte with Superior Dimensional Stability for Alkaline Fuel Cell Membranes. *J. Mater. Chem. A* **2015**, *3* (25), 13350–13356. https://doi.org/10.1039/c5ta02304a.

(55) Demitri, C.; Del Sole, R.; Scalera, F.; Sannino, A.; Vasapollo, G.; Maffezzoli, A.; Ambrosio, L.; Nicolais, L. Novel Superabsorbent Cellulose-Based Hydrogels Crosslinked with Citric Acid. *J. Appl. Polym. Sci.* **2008**, *110* (4), 2453–2460. https://doi.org/10.1002/app.28660.

(56) Olsson, E.; Hedenqvist, M. S.; Johansson, C.; Järnström, L. Influence of Citric Acid and Curing on Moisture Sorption, Diffusion and Permeability of Starch Films. *Carbohydr. Polym.* **2013**, *94* (2), 765–772. https://doi.org/10.1016/j.carbpol.2013.02.006.

(57) Sharma, P. R.; Joshi, R.; Sharma, S. K.; Hsiao, B. S. A Simple Approach to Prepare Carboxycellulose Nanofibers from Untreated Biomass. *Biomacromolecules* **2017**, *18* (8), 2333–2342. https://doi.org/10.1021/acs.biomac.7b00544.

(58) Sharma, P. R.; Zheng, B.; Sharma, S. K.; Zhan, C.; Wang, R.; Bhatia, S. R.; Hsiao, B. S. High Aspect Ratio Carboxycellulose Nanofibers Prepared by Nitro-Oxidation Method and Their Nanopaper Properties. *ACS Appl. Nano Mater.* **2018**, *1* (8), 3969–3980. https://doi.org/10.1021/acsanm.8b00744.

(59) Isogai, A.; Saito, T.; Fukuzumi, H. TEMPO-Oxidized Cellulose Nanofibers. *Nanoscale* **2011**, *3* (1), 71–85. https://doi.org/10.1039/C0NR00583E.

(60) Fukuzumi, H.; Saito, T.; Iwata, T.; Kumamoto, Y.; Isogai, A. Transparent and High Gas Barrier Films of Cellulose Nanofibers Prepared by TEMPO-Mediated Oxidation. *Biomacromolecules* **2009**, *10* (1), 162–165. https://doi.org/10.1021/bm801065u.

(61) Saito, T.; Isogai, A. TEMPO-Mediated Oxidation of Native Cellulose. The Effect of Oxidation Conditions on Chemical and Crystal Structures of the Water-Insoluble Fractions. *Biomacromolecules* **2004**, *5* (5), 1983–1989. https://doi.org/10.1021/bm0497769.

(62) Ruland, W. X-Ray Determination of Crystallinity and Diffuse Disorder Scattering. *Acta Crystallogr.* **1961**, *14* (11), 1180–1185. https://doi.org/10.1107/S0365110X61003429.

(63) Segal, L.; Creely, J. J.; Martin, A. E.; Conrad, C. M. An Empirical Method for Estimating the Degree of Crystallinity of Native Cellulose Using the X-Ray Diffractometer. *Text. Res. J.* **1959**, *29* (10), 786–794. https://doi.org/10.1177/004051755902901003.

(64) Park, S.; Baker, J. O.; Himmel, M. E.; Parilla, P. A.; Johnson, D. K. Cellulose Crystallinity Index: Measurement Techniques and Their Impact on Interpreting Cellulase Performance. *Biotechnol. Biofuels* **2010**, *3* (1), 10. https://doi.org/10.1186/1754-6834-3-10.

(65) Shi, R.; Zhang, Z.; Liu, Q.; Han, Y.; Zhang, L.; Chen, D.; Tian, W. Characterization of Citric Acid/Glycerol Co-Plasticized Thermoplastic Starch Prepared by Melt Blending. *Carbohydr. Polym.* **2007**, *69* (4), 748–755. https://doi.org/https://doi.org/10.1016/j.carbpol.2007.02.010.

(66) Ornaghi Júnior, H. L.; Zattera, A. J.; Amico, S. C. Thermal Behavior and the Compensation Effect of Vegetal Fibers. *Cellulose* **2014**, *21* (1), 189–201. https://doi.org/10.1007/s10570-013-0126-x.

(67) Mali, K. K.; Dhawale, S. C.; Dias, R. J.; Dhane, N. S.; Ghorpade, V. S. Citric Acid Crosslinked Carboxymethyl Cellulose-Based Composite Hydrogel Films for Drug Delivery. *Indian J. Pharm. Sci.* **2018**, *80* (4), 657–667. https://doi.org/10.4172/pharmaceutical-sciences.1000405.

(68) Wyrzykowski, D.; Hebanowska, E.; Nowak-Wiczk, G.; Makowski, M.; Chmurzyński, L. Thermal Behaviour of Citric Acid and Isomeric Aconitic Acids. *J. Therm. Anal. Calorim.* **2011**, *104* (2), 731–735. https://doi.org/10.1007/s10973-010-1015-2.

(69) Wang, M.; Shao, C.; Zhou, S.; Yang, J.; Xu, F. Preparation of Carbon Aerogels from TEMPO-Oxidized Cellulose Nanofibers for Organic Solvents Absorption. *RSC Adv.* **2017**, *7* (61), 38220–38230. https://doi.org/10.1039/C7RA05506D.

(70) Kim, H.; Guccini, V.; Lu, H.; Salazar-Alvarez, G.; Lindbergh, G.; Cornell, A. Lithium Ion Battery Separators Based on Carboxylated Cellulose Nanofibers from Wood. *ACS Appl. Energy Mater.* **2019**, *2* (2), 1241–1250. https://doi.org/10.1021/acsaem.8b01797.

(71) Qiao, J.; Yoshimoto, N.; Morita, M. Proton Conducting Behavior of a Novel Polymeric Gel Membrane Based on Poly(Ethylene Oxide)-Grafted-Poly(Methacrylate). *J. Power Sources* **2002**, *105* (1), 45–51. https://doi.org/10.1016/S0378-7753(01)00963-6.

导师简历

Miriam Rafailovich

Distinguished Professor and Undergraduate Program Co-director (CME)

Office: 322 Engineering Bldg. Stony Brook, NY

Phone: 516-458-9011

Email: Miriam.Rafailovich@stonybrook.edu

Surface and interface properties of polymer thin films, nanocomposite materials, phase segregation in polymer blends, polymer dynamics in confined geometries, wetting in multilayer polymer films, fracture toughness of polymer interfaces, polymer adhesion, nanopatterning using polymer self assembly, nanotribiology of polymer film surfaces, nanopatterning with magnetic impregnates in glass. Experimental specialization: SIMS, X-ray and Neutron Reflection, Lateral, magnetic and atomic force microcopy TEM, RBS, and Mossbauer Spectroscopy.

Honors

- Co- Director NSF Materials Research Science & Engineering Center: Polymers at Engineered Interfaces
- SUNY Chancellors Award for Research in Science, Engineering, and Medicine
- Fellow, American Physical Society
- Siemens Foundation Recognition Award as Outstanding Mentor for the Westinghouse, Competition in Math, Science, and Technology

Education

- PhD, Nuclear Physics, 1981, SUNY Stony Brook, USA.
- BS, Physics and Biology, 1975, Brooklyn College, USA.

Career

- Distinguished Professor, 2007-present, SUNY at Stony Brook.
- Distinguished Professor, 2007-present, SUNY at Stony Brook.
- Professor, 1992-2007. SUNY at Stony Brook.
- Lady Davis Visitor, 2006-2007, Hebrew University.
- Professor, 1992-94,Queens College.
- Associate Professor, 1988-92, Queens College.
- Guest Scientist, 1987-Present, Brookhaven National Lab.
- Senior Scientist, 1985-88,Weizmann Institute.
- Research Associate, 1984-85,Weizmann Institute.
- Visiting Assistant Physicist, 1982-84,Brookhaven National Lab.
- Research Associate, 1980-82, SUNY at Stony Brook.